fib WILEY

A limit state design approach for hybrid reinforced concrete column-supported flat slabs

Stanislav Aidarov[1,2] | Nikola Tošić[2] | Albert de la Fuente[2]

[1]Smart Engineering Ltd, UPC Spin-Off, Barcelona, Spain

[2]Department of Civil and Environmental Engineering, Universitat Politècnica de Catalunya (UPC), Barcelona, Spain

Correspondence
Albert de la Fuente, Jordi Girona 1-3, Barcelona, 08034, Spain.
Email: albert.de.la.fuente@upc.edu

Funding information
Departament d'Innovació, Universitats i Empresa, Generalitat de Catalunya, Grant/Award Number: 2018 DI 77; Ministerio de Ciencia e Innovación, Grant/Award Number: CREEF (PID2019-108978RB-C32)

Abstract

Hybrid reinforced technology (combination of steel reinforcing bars and fibers) can be considered as a competitive alternative to the already existing solutions for the construction of column-supported flat slabs. Constructed hybrid-reinforced buildings prove that hybrid solutions have sufficient bearing capacity to maintain structural integrity despite being exposed to high stress levels, thereby providing a beneficial solution in terms of toughness, ductility, and sustainability performance. However, the lack of design-oriented recommendations based on the accepted limit state format for dealing with both serviceability and ultimate limit states slows down the wider implementation of this technology. Considering the above-mentioned, this article presents a simplified design-oriented method that covers the evaluation of the structural response of hybrid reinforced concrete column-supported flat slabs in terms of flexural strength, cracking, and instantaneous deformations. Two hybrid reinforced alternatives for a given flat slab are studied by means of the proposed approach. Furthermore, a nonlinear finite element analysis is carried out in order to evaluate the effectiveness of the developed simplified method. Based on the achieved results, its suitable accuracy and precision can be pointed out. This outcome may motivate current practitioners to consider hybrid reinforced concrete solutions as a possible alternative during the design of residential and office buildings.

KEYWORDS
cracking control, deflection, elevated slab, fiber reinforced concrete, flexure, FRC, serviceability behavior, two-way slab, ultimate behavior

1 | INTRODUCTION

During the last two decades, considerable scientific efforts have been made to identify and quantify the full potential of fiber reinforced concrete (FRC) and hybrid reinforced concrete (combination of steel reinforcing bars and fibers, HRC) slabs in statically redundant structures.

Numerous laboratory tests were carried out, varying the fiber/rebar content, slab geometry, boundary, and load conditions.[1-7] The obtained results highlighted the enhanced structural response in terms of ductility,[3,6,7] cracking control,[1,2,5] and load redistribution.[1,5,7]

Real-scale testing of elevated flat slabs confirmed the possibility of even total substitution of traditional reinforcement through using fibers in the concrete mix, this providing sufficient and even enhanced flexural and punching strength.[8-13] The promising capability of FRC technology was also confirmed in real projects: significant benefits in terms of construction time and costs were highlighted during the construction of the Ditton Nams shopping mall (Latvia), the Triangle office building (Estonia), the Rocca Al-Mare office tower (Estonia), and the LKS office building (Spain).[14-16]

Despite the successful experiences of FRC slab construction, a number of shortcomings were revealed under special structural and/or construction conditions. The total substitution of traditional reinforcement by FRC can be inefficient if the bending and shear stresses magnitudes differ significantly throughout the slab. This variation requires different residual tensile strength (f_R) of the FRC and, as a consequence, different amount of fibers in different areas of the slab. In this sense, FRC has to be designed for guaranteeing the most demanding f_R requirement; this strategy will provide over-reinforced areas and uncompetitive solutions.

Another drawback of FRC is the slight material heterogeneity within the depth of the element[8]; the tendency of an increase in the fiber content towards the lower layers of the slab[9,17] can lead to insufficiently controlled cracks in the zones with high negative bending moments (in the vicinity of the columns). Considering these aspects, hybrid solutions might be even more attractive from technical and economic points of view since moderate values of f_R can be imposed while most demanding bending and punching forces can be resisted by the combination of fibers and steel bars—enhancing also the workability of the concrete due to reduction of the fiber content in the mix.

Although the use of FRC and HRC in elevated flat slabs evidenced encouraging results, these alternatives are barely considered by engineers within the design process of residential and office buildings despite the acceptance of using FRC in structural elements by national and international codes along with specific guidelines.[18-23] One of the main reasons, apart from general concerns regarding the material capacity, is the lack of a detailed description on how to cover all the limit states for FRC/HRC flat slab design. Even scientific literature do not cover all required design aspects for this type of structural elements. In this regard, Table 1 shows that the majority of works are focused on the behavior of FRC/HRC elevated slabs at the ultimate limit state (ULS), providing the analytical and numerical approaches to assess the flexural and/or punching strength of the studied structural element.

In this context, the frequent questions of design engineers, which are hindering the widespread use of FRC/HRC in column-supported flat slabs, can be summarized as the following:

- How should the cracking behavior of FRC/HRC elevated flat slab be estimated at the serviceability limit state (SLS)?
- What is the most appropriate way to assess the deformations of FRC/HRC flat slabs?
- Does the FRC/HRC approach provide adequate results with respect to long-term behavior?
- What is a suitable method to carry out a comparison between traditional and FRC/HRC solutions?

Most of the questions can actually be answered by means of nonlinear finite element analysis (NLFEA). The existing scientific literature (Table 1) evidences the capacity to properly predict the structural response of two-way slabs using nonlinear finite element models.[36,38,41] Moreover, a NLFE parametric studies were carried out in order to analyze the structural response of the different FRC/HRC alternatives.[37] However, the application of these models is infrequent among structural designers since: (1) appropriate software to perform these analyses are not meant for day-to-day design procedures and (2) the lack of thoroughly described approaches for nonlinear analysis in current codes and guidelines for this specific purpose.

Taking this into account, this article presents a simplified method for the design of FRC/HRC elevated slabs which responds to the majority of above-presented questions. This method permits the evaluation of the flexural capacity of the structural elements at ULS and the analysis of their response in terms of cracking and instantaneous deformations at SLS. Moreover, the developed approach allows checking the required ductility of FRC/HRC column-supported flats slabs. Based on the proposed design procedure, HRC solutions were analyzed for the given structure and the obtained results were compared with those obtained by NLFEA.

2 | PROPOSED DESIGN APPROACH

2.1 | Flexural ULS bearing capacity

2.1.1 | Basis of the yield line method

The Yield Line Method (YLM) is being frequently suggested to evaluate the flexural load-carrying capacity

of FRC flat slabs owing to its representativeness and the ease of application (very few restrictions).[18] These restrictions, that exist for elasticity-based methods, are related to the boundary conditions, opening dimensions and load types along with the possibility of taking into account the ductility/rotation capacity of FRC—the essential parameter to use the plastic analysis methods. YLM is also a suitable analytical approach to design RC slabs, as long as the required ductility can be proven by limiting the area of tensile reinforcement so that the following limits are fulfilled: $x/d \leq 0.25$ and $x/d \leq 0.15$ for concrete strength classes $\leq$ C50/60 and $\geq$ C55/67, respectively.[19,42] Taking into account that flat slabs typically have low ratios of tensile reinforcement ($\rho_s = A_s/(b \cdot d)$), the abovementioned restrictions are to be generally fulfilled.

YLM is based on Johansen's theory[43–45] and claims that the ultimate load of a slab can be obtained by postulating a collapse mechanism (generated by yield lines) that is compatible with boundary conditions. The selection of the collapse mechanism is of paramount importance considering that its wrong estimation will lead to the theoretically unsafe results since the presented method gives upper bound solutions. However, yield line patterns have been developed and thoroughly studied for common geometries (Figure 1). Additionally, the standard formulae are already developed for these geometries in order to directly calculate the relation between applied load and produced moments per unit length ($m_{Ed,YL}^+, m_{Ed,YL}^-$); otherwise, such ratios can be found by means of segmental equilibrium or method of virtual work.[18,45,47]

In case of a column-supported flat slabs with a common column grid which is subjected to uniformly distributed load (UDL), three "applied load–produced design moment" relationships are to be assessed by means of standard formulae. Two of these refer to, so-called, global

failure of internal (Equation 1) and corner (Equation 2) panels of the slab (Figure 1a), whereas the third case concerns local failure (Figure 1b)—the situation where the ultimate load is transferred to the column from the slab tributary area.[18] Equation 3 presents "concentrated load-produced design moment" relationship for the internal column, whereas Equation 4 covers the general case for the perimeter columns with an unknown angle (ω, in [rad])[46–48] which is equal to π or $\pi/2$ for edge and corner columns, respectively. Importantly, these equations permit to vary the ratio of support to mid span moments ($\oslash_h$, Equation 5) as long as the ductility requirement is respected.

$$m_{Ed,YL}^+ = \frac{q_d \cdot L_{rx}^2}{8 \cdot (1 + \oslash_h)} \tag{1}$$

$$m_{Ed,YL}^+ = \frac{q_d \cdot L_{ry(x)}^2}{2\left(\sqrt{(1 + \oslash_h)} + 1\right)^2} \tag{2}$$

$$m_{Ed,YL}^+ = P \cdot \left(1 - \sqrt[3]{\frac{q_d \cdot A}{P}}\right) \Big/ 2\pi \cdot (1 + \oslash_h) \tag{3}$$

$$m_{Ed,YL}^+ = P \cdot \left(1 - \sqrt[3]{\frac{q_d \cdot A}{P}}\right) \Big/ (\omega \cdot (1 + \oslash_h) - 1.14 \cdot \oslash_h) \tag{4}$$

$$\oslash_h = m_{Ed,YL}^- \Big/ m_{Ed,YL}^+ \tag{5}$$

2.1.2 | Flexural strength of HRC: Sectional model

Currently, the majority of codes[19,21,22] suggest the simplified rigid plastic model for the assessment of the ULS behavior of FRC in tension which is identified by a

TABLE 1 Previous research focused on design of FRC/HRC elevated flat slabs

| References | Analytical or numerical approaches | | | | |
	Flexural strength	Punching strength	Cracking	Instant deformations	NLFEA
Destrée & Mandl[10]; di Prisco et al.,[2]; di Prisco et al.,[24]; Maturana et al.,[25]; Michels et al.,[6]	●				
Choi et al.,[26]; Gouveia et al.,[27]; Higashiyama et al.,[28]; Ju et al.,[29]; Kueres et al.,[30]; Maya et al.,[31]; Nguyen-Minh et al.,[32]; Yang et al.,[33]		●			
Barros et al.,[34]; Tan & Venkateshwaran,[35]	●	●			
Gödde & Mark,[36]; Nogales & de la Fuente,[37]; Salehian & Barros,[38]; Soranakom & Mobasher,[39]; Teixeira et al.,[40]					●
Barros et al.,[9]; Facconi et al.,[41]; Salehian & Barros,[17]	●				●
Present Study	●	●	●	●	●

unique value of f_{Ftud}. This can be based on the characteristic residual tensile strength at the crack mouth opening displacement (CMOD) of 2.5 mm (f_{R3k}) according to EN 14651[49] and can be calculated as $f_{Ftud} = f_{R3k}/(3 \cdot \gamma_F)$, where $\gamma_F = 1.50$ is the partial safety factor in tension for FRC. Taking into account this model, the *fib* MC 2010[19] suggests to evaluate the design resisting moment of FRC ($m_{Rd,FRC}$) by concentrating the whole compressive force in the top fiber of the section, disregarding the traditionally adopted compressive block. However, considering the appearance of relatively high stresses in certain zones of column-supported slabs, the neutral axis may be fixed at 10% of the element thickness for all studied sections in order to provide a safer design procedure; thus, $m_{Rd,FRC} = 0.45 \cdot f_{Ftud} \cdot h^{2}$.[16]

The design resisting moment of HRC ($m_{Rd,HRC}$) could be evaluated complementing the above described sectional analysis by the presence of additional force provided by steel reinforcing bars ($A_s \cdot f_{yd}$). However, the more convenient way is to estimate $m_{Rd,HRC}$ as depicted in Figure 2, i.e., the total flexural strength corresponds to the sum of separately calculated $m_{Rd,FRC}$ and $m_{Rd,RC}$ where the latter is the design resisting moment of traditionally reinforced concrete.[50] This approach permits to compute the maximum design moments (m_{Ed}) in the critical areas (Section 2.1.3) and after calculating the contribution of fibers ($m_{Rd,FRC}$), assess the requirement of reinforcing bars as if it were traditionally reinforced concrete in every section which satisfies the following condition: $m_{Rd,RC} = m_{Ed} - m_{Rd,FRC} \geq 0$.

Nevertheless, the neutral axis can be found below 10% of the element thickness which will lead to an overestimation of the flexural strength of the section using the simplified sectional model (Figure 2). Therefore, for the cases where more accurate results are demanded, the essential sectional parameters for both FRC and HRC can be computed by imposing sectional force equilibrium and deformation compatibility conditions in accordance with models presented in Figure 3. These parameters permit to assess the bearing capacity of the two-way system (providing more accurate outcomes in comparison with the previously suggested approach, Figure 2) based on the procedure described in the Section 2.1.3.

The above-described models are currently used within the analytical design procedure of FRC two-way slabs. However, the recent studies revealed that the implementation of those could be complemented by the introduction of structural redistribution factor[51,52] and/or orientation factor[53–55] in order to ensure the more accurate evaluation of the structural response in flexure. The magnitude of the former (up to 1.4) depends on the redistribution capacity of the studied element, whereas the latter takes into account the orientation of fibers which, in turn, is influenced by the rheological properties of concrete, casting method, and the geometry of the element in question.[56]

2.1.3 | YLM for HRC flat slabs

The difference between FRC and HRC column-supported flat slab design by means of YLM consists of certain challenges in the correct proportioning of the stresses along
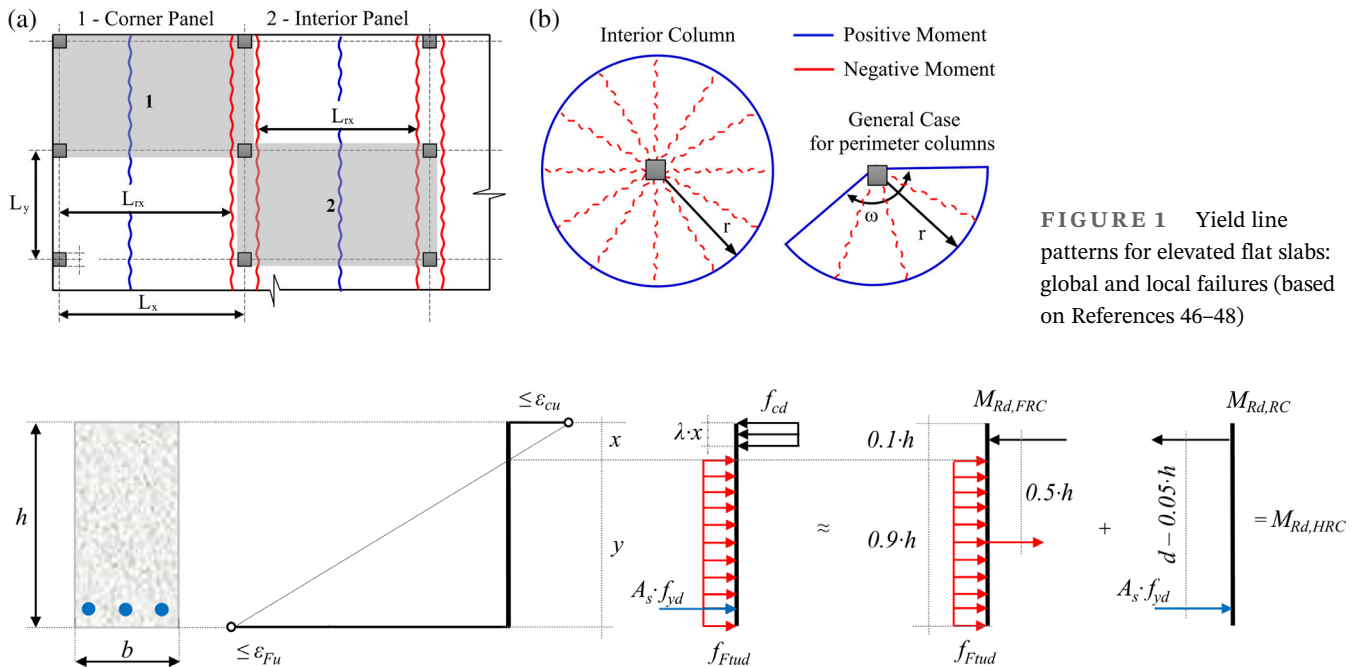

FIGURE 1 Yield line patterns for elevated flat slabs: global and local failures (based on References 46–48)

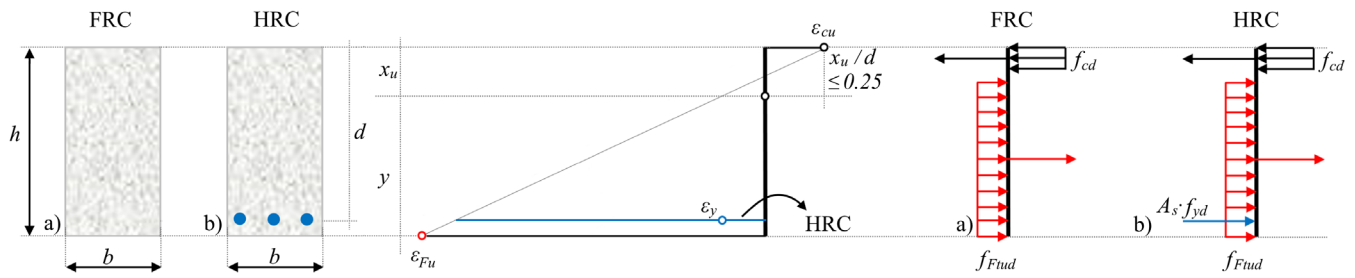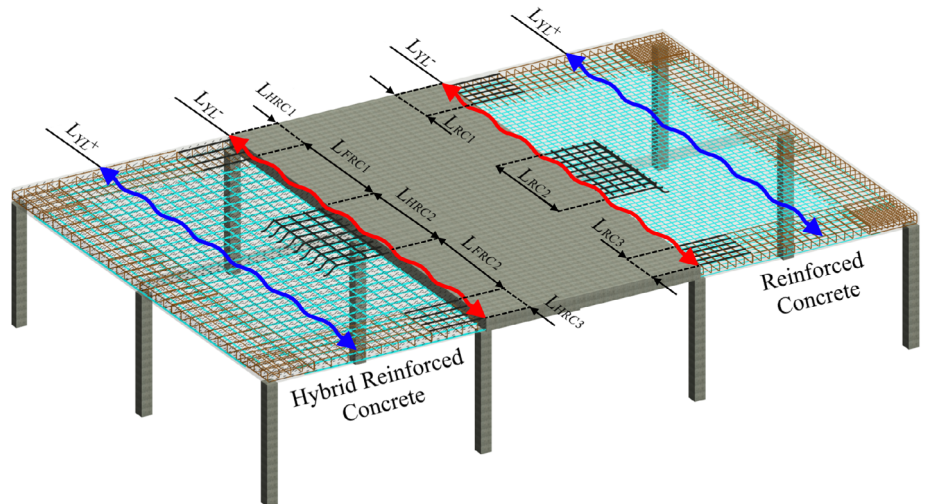**FIGURE 2** Simplified sectional model to assess flexural strength of HRC

FIGURE 3 Sectional models to assess flexural strength of (a) FRC and (b) HRC

FIGURE 4 Yield line pattern for the global failure mode: HRC and RC solutions

the yield lines in the latter case, taking into account the possible variety in reinforcement layouts.[41] However, drawing an analogy to the design of RC flat slabs by YLM, the procedure does not differ significantly. Once the geometry, reinforcement layout, and load conditions are established, the ratio of support to mid span moments ($\oslash_h$) is to be chosen to calculate maximum design moments per unit length for the global failure mode.

The slight difference arises in the following step, when the required traditional reinforcement shall be computed in accordance with (1) considered layout and (2) maximum design moments along the yield lines. Firstly, the required amount of the reinforcing bars can be calculated for the bottom reinforcement. Taking into account that, in accordance with YLM, the curtailment is not advisable for the latter, the procedure is straightforward: the simplified approach (Figure 2) or accurate sectional analysis (Figure 3) can be applied. In turn, the top reinforcement is frequently found curtailed; therefore, the need of design moment proportioning should be considered.

In case of RC flat slabs (Figure 4), the task can be performed by means of Equation 6: multiplying the calculated moment (Equations 1 and 2) by the length of the yield line (L_{YL}) and dividing the obtained value by

the length along the same yield line which is covered by the top reinforcement.[47] The presence of fibers in the concrete mix modifies the above described procedure; Equation 7 provides the consideration of its contribution to the flexural strength and, as a consequence, the design bending moment which shall be resisted by reinforcing bars in accordance with the simplified model presented in Figure 2. The more accurate procedure demands to find the resisting moment of the FRC section (Figure 3a) with following proportioning of the design bending moment to the HRC zones by means of Equation 8 (Figure 4). The obtained magnitude of this moment permits to compute the required amount of the reinforcing bars using the sectional model presented in Figure 3b. Finally, the verification of the sufficient flexural strength against local flexural failure modes shall be performed for both cases in order to complete the analysis (the detailed description of the method implementation is provided in the Supporting Information available with the online version of the article, Appendix S1).

$$m_{Ed}^- = \frac{m_{Ed,YL}^- \cdot L_{YL^-}}{\sum L_{RC_i^-}} \quad (6)$$

$$m_{\mathrm{Ed,RC}}^{-} = \frac{\left(m_{\mathrm{Ed,YL}}^{-} - m_{\mathrm{Rd,FRC}}\right) \cdot L_{\mathrm{YL}^{-}}}{\sum L_{\mathrm{HRC}_i^{-}}} \quad (7)$$

$$m_{\mathrm{Ed,HRC}}^{-} = \frac{m_{\mathrm{Ed,YL}}^{-} \cdot L_{\mathrm{YL}^{-}} - m_{\mathrm{Rd,FRC}} \cdot \sum L_{\mathrm{FRC}_i^{-}}}{\sum L_{\mathrm{HRC}_i^{-}}} \quad (8)$$

2.2 | Structural response of HRC flat slabs at SLS

2.2.1 | Internal forces and reinforcement distribution

In already constructed HRC flat slabs, generally, the absence of cracking under quasi-permanent load combinations was pointed out which permitted to evaluate the produced deformations as for an isotropic linear elastic material.[15,25] However, the presence of cracks in this type of elements is expectable—in accordance with ACI 421.3R-15, microcraking in two-way concrete slabs starts at an early level of approximately 10% of the service load, whereas the pattern of potential yield lines is almost fully developed at 30% of the same load.[57]

Therefore, straightforward analytical methods are required to evaluate the response of HRC in terms of cracking and deformations. This is not a trivial task considering that even the behavior of RC two-way slabs at SLS still demands further studies and seems to be significantly more complex than the cases related to beams and/or one-way plates. Additionally, the proposed methods should be correlated with the current codes and guidelines in order to be used by practitioners. With this in mind, the approach based on the analogy with RC flat slabs design is presented herein; the overarching goal is to prove that HRC solutions comply with minimum requirements described in the *fib* MC 2010[19] and Eurocode 2 (EC2)[42] for traditionally reinforced alternative.

To this end, several additional steps, which are not directly dealing with the HRC flat slab design process, are to be carried out: (1) divide the given structure into column and middle strips (Figure 5a) pursuant to current regulations[18,22,42] and (2) simplify the regular elastic distribution of moments (Figure 5b) at ULS by means of the Direct Design Method (DDM) or Equivalent Frame Method (EFM, Figure 5c). The same procedure can be performed by finite element analysis, averaging the moments within each strip in order to obtain constant moments in critical sections (in the vicinity of columns and at mid-spans). The obtained information will serve as a basis for further design assumptions which are described in Sections 2.2.2 and 2.2.3.
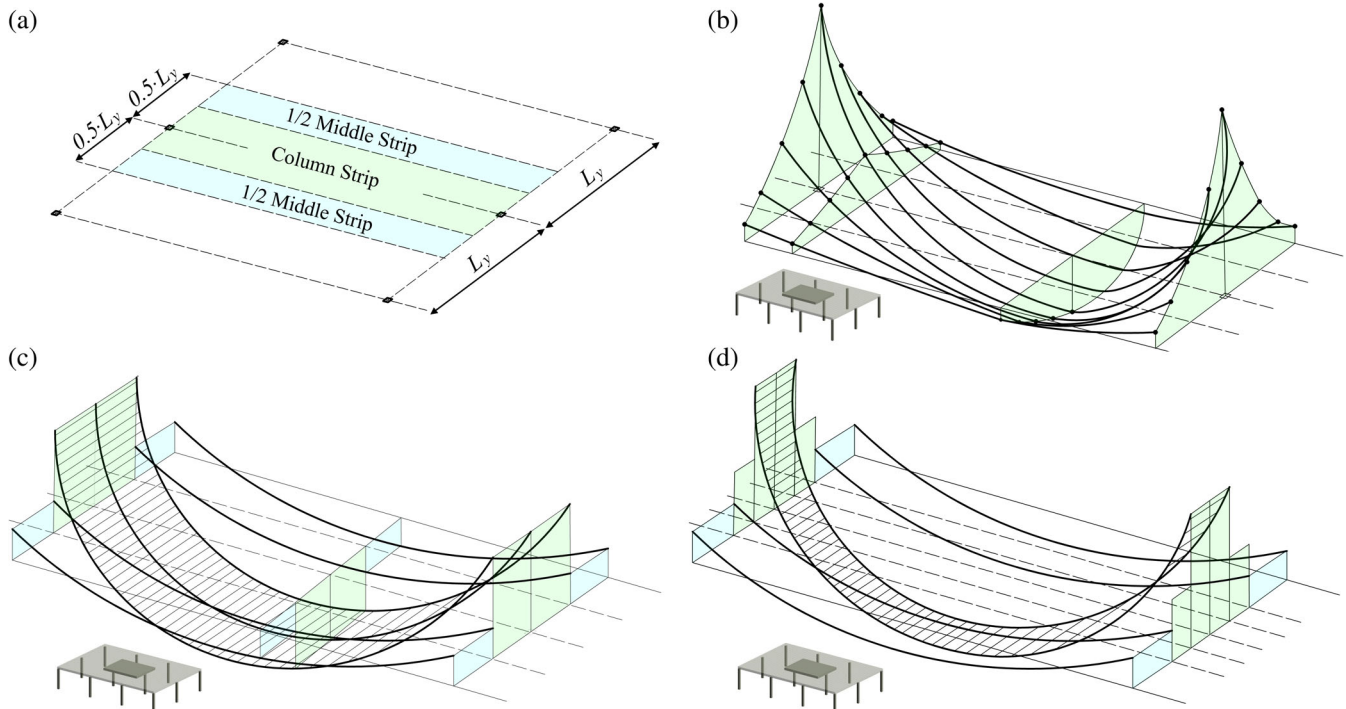

FIGURE 5 (a) Division of flat slab into column and middle strips; (b) typical elastic moment distribution under UDL; (c) moment distribution according to DDM/EFM; and (d) adjustments of moment distribution to meet SLS requirements (adapted from Reference 58)

2.2.2 | Cracking control

Generally, the indirect control of cracking is widely applied for RC slabs subjected to bending without significant axial tension, i.e., respecting the established values of maximum permitted steel stresses and reinforcing bar diameter/spacing.[19] In case of RC flat slabs, specific suggestions regarding the detailing of the reinforcement can be found in different studies and regulations. For instance, EC2[42] states that at internal columns, 50% of the reinforcement, which is required to resist the full negative moment from the sum of the two half panels each side of the column, should be placed in a width equal to the sum of 0.125 times the panel width on either side of the column. Similarly, the works of Jofriet[59] and Brotchie et al.[60] propose the division of the negative column strip into two strips of equal length. Further, the inner negative column strip is to be designed for two-thirds of the total negative column strip moment in order to meet SLS requirements.

The demand for more rigorous calculations can be accompanied with a number of constraints. ACI Codes,[57,61,62] for instance, consider that crack control equations for beams underestimate the crack widths developed in two-way slabs, drawing on the scientific works developed, mainly, by Nawy.[63,64] However, the development of this expression was formulated for cracks produced mainly in positive-moment regions, i.e., the regions with clear two-way bending. In turn, cracks tend to appear in the vicinity of columns under the quasi-permanent combination of actions in column-supported flat slabs,[65] therefore, it might be important to note that the one-way bending is predominant at faces of the columns.

Referring the above described information to HRC flat slabs, it is evident that further experimental tests along with the validation of existing models are necessary for the accurate assessment of maximum crack widths in column-supported flat slabs. Therefore, being conservative, the methods related to indirect control of cracking in RC column-supported flat slabs can be adapted to HRC solutions, assuring that the latter is not inferior to the RC alternative.

For that purpose, first, the maximum design moment above the columns computed by DDT/EFM (Figure 5c) is to be modified in accordance with EC2[42] (Figure 5d). In fact, EC2[42] provides this re-proportioning in terms of required top reinforcement area; however, the same relationship can be presented in terms of ultimate flexural moments for the sake of more direct design procedure (with minor difference in the overall result). Based on the modified moment, the required amount of the reinforcement for RC solution is to be assessed—the obtained result permits to omit the subsequent verification of the structure at limit state of cracking according to EC2.[42] Eventually, the steel stresses can be evaluated in the RC section above the columns as for a continuous beam with a unit width (1000 mm) and the depth equal to the thickness of the slab (h).

A similar procedure should be repeated for HRC solution. Basing on the FRC properties along with the reinforcement layout, the required amount of steel bars is to be found by means of YLM (Section 2.1). Thereafter, the steel stresses in the critical sections should be estimated, considering the same dimensions ($h \times 1000$ mm). For more detailed analysis of FRC contribution to the structural response of the HRC section at SLS, the multilinear constitutive model in tension (Figure 6) shall be applied.[19] The majority of variables for this model depend on the mean residual tensile strengths at CMODs of 0.5 mm (f_{R1m}), 2.5 mm (f_{R3m}) according to EN 14651[49] and can be computed as follows: (1) $f_{ct} = 0.30 \cdot (f_{ck})^{2/3}$; (2) $f_{Ftsm} = 0.45 \cdot f_{R1m}$; (3) $f_{Ftum} = f_{Ftsm} - (w_u/CMOD_3) (f_{Ftsm} - 0.5 \cdot f_{R3m} + 0.2 \cdot f_{R1m})$; (4) $\varepsilon_{SLS} = CMOD_1/l_{cs}$; (5) $\varepsilon_{ULS} = w_u/l_{cs} = \min (\varepsilon_{Fu}, 2.5/l_{cs} = 2.5/y)$; (6) $\varepsilon_{Fu} = 20‰$ (considering variable strain distribution along the cross section).

The computed sectional parameters for both RC and HRC should be used to check the sufficient cracking control of the latter by means of two approaches: (1) comparing the achieved stresses (more conservative method) or (2) computing the crack widths as for one-way elements.
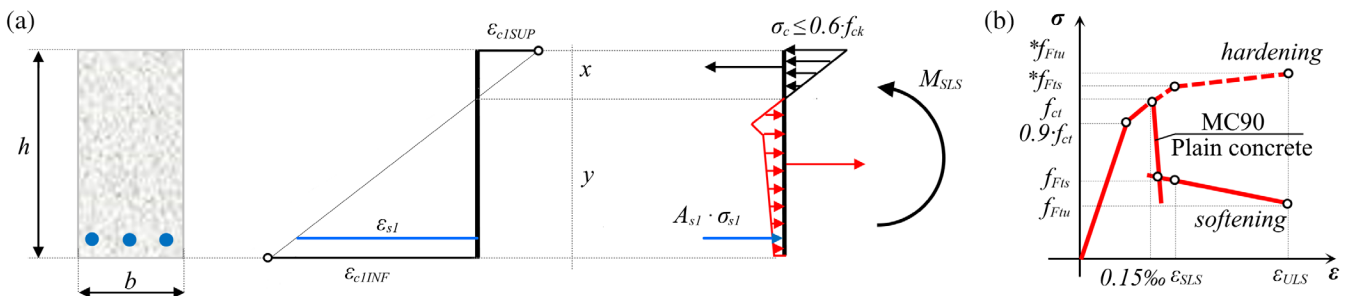

FIGURE 6 Sectional model to assess steel stresses in cracked sections (adapted from Reference 66)

Conservatively, the steel stresses in each section should be compared and, in case of $\sigma_{s,HRC} \leq \sigma_{s,RC}$, HRC solution presents at least the same performance in terms of cracking control in comparison with RC alternative owing to the fact that the presence of fibers in the material enhances the bond between steel bars and concrete. This phenomenon leads to the reduction of the bond transfer length and, as a result, crack spacing.[67-69] The reduction of crack spacing will ensure a minor crack width in the HRC alternative for the same magnitudes of steel stresses (strains).

Otherwise ($\sigma_{s,HRC} \geq \sigma_{s,RC}$), the chosen reinforcement layout for ULS (YLM) can be unevenly distributed within the column strip pursuant to EC2[42] in order to reduce the steel stresses up to the required magnitude. However, it is important to consider the necessity to keep the required flexural strength in the column strip outside the mentioned area (Figure 5d). The described case is not likely to occur in the HRC solution with moderate fiber content since YLM allows to concentrate the rebar layout in the vicinity of columns (Figure 4) and, as a consequence, lead to considerable values of negative moments in these zones.[47] Nevertheless, by increasing the fiber content, the negative moments along the yield line will be more uniformly distributed, i.e., less traditional reinforcement in the form of steel bars is required. Therefore, the verification of sufficient crack control might be necessary and can be assured even by placement of the additional steel bars in the centre part of the column strip.

Alternatively, the crack widths can be assessed in the critical sections as for one-way elements.[65] The design crack width for the RC solution can be evaluated by means of Equations 9–13 in accordance with the *fib* MC 2010 (Clause 7.6.4.4).[19] The same equations are valid for the analysis of HRC—for that purpose, provided f_{ctm} is to be substituted by $f_{ctm}-f_{Ftsm}$ in Equations 10 and 12, taking into account the effect of fibers on the transfer length. Thereafter, the comparative procedure is identical with the one related to the analysis of the produced steel stresses. Summarizing, Figure 7 highlights the essential steps to justify the appropriate structural response of HRC column-supported flats slabs at limit states of cracking for both approaches.

$$w_d = 2 \cdot l_{s,max} \cdot (\varepsilon_{sm} - \varepsilon_{cm} - \varepsilon_{cs}) \tag{9}$$

$$l_{s,max} = k \cdot c + \frac{1}{4} \cdot \frac{f_{ctm}}{\tau_{bms}} \cdot \frac{\O_s}{\rho_{s,ef}} \tag{10}$$

$$\varepsilon_{sm} - \varepsilon_{cm} - \varepsilon_{cs} = \frac{\sigma_s - \beta \cdot \sigma_{sr}}{E_s} - \eta_r \cdot \varepsilon_{sh} \tag{11}$$
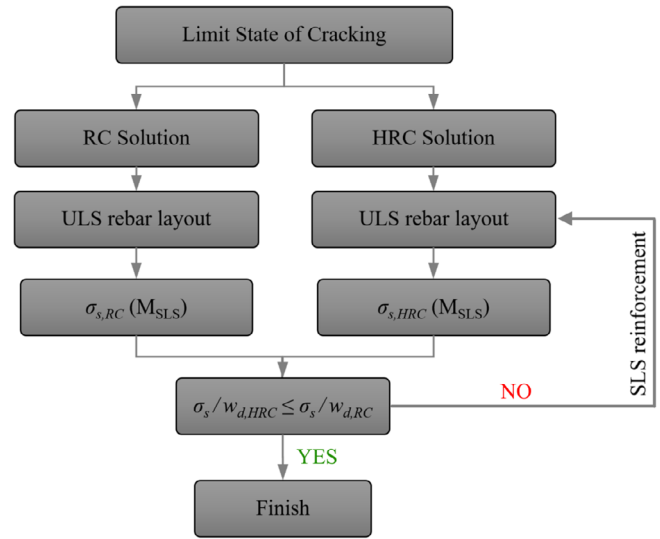

FIGURE 7 Flowchart to present the sufficient crack control of HRC solutions in column-supported flat slabs

$$\sigma_{sr} = \frac{f_{ctm}}{\rho_{s,ef}} \cdot \left(1 + \alpha_e \cdot \rho_{s,ef}\right) \tag{12}$$

$$\rho_{s,ef} = \frac{A_s}{A_{c,ef}} \tag{13}$$

2.2.3 | Instantaneous deformations

The design of elevated slabs is typically governed by the deflection control[70] and the correct evaluation of this aspect is of a paramount importance given that this structural element constitute 80–90% of the total cost of a concrete frame.[71] Moreover, it is also important to highlight that the flexural strength for the studied case is to be assessed by means of YLM—approach that provides suitable results for ULS, but does not provide information for serviceability design.[65]

With this in mind, simplified analysis methods for RC solutions are adapted herein in order to evaluate the magnitude of deflections in HRC column-supported flats slabs (Figure 8). Several methods were studied[72-77] and the approach to calculate deflections by means of crossing beam analogy was chosen as this providing: (1) relatively simple design procedure and (2) significant correlation with experimental data.[71,75,76] Importantly, the presence of fibers as reinforcing material is compatible with this design procedure. Moreover, that has a potential to be extended in order to assess the long-term response of the FRC structural elements—the aspect of the paramount importance that still requires further research[78] and is beyond the scope of this article.
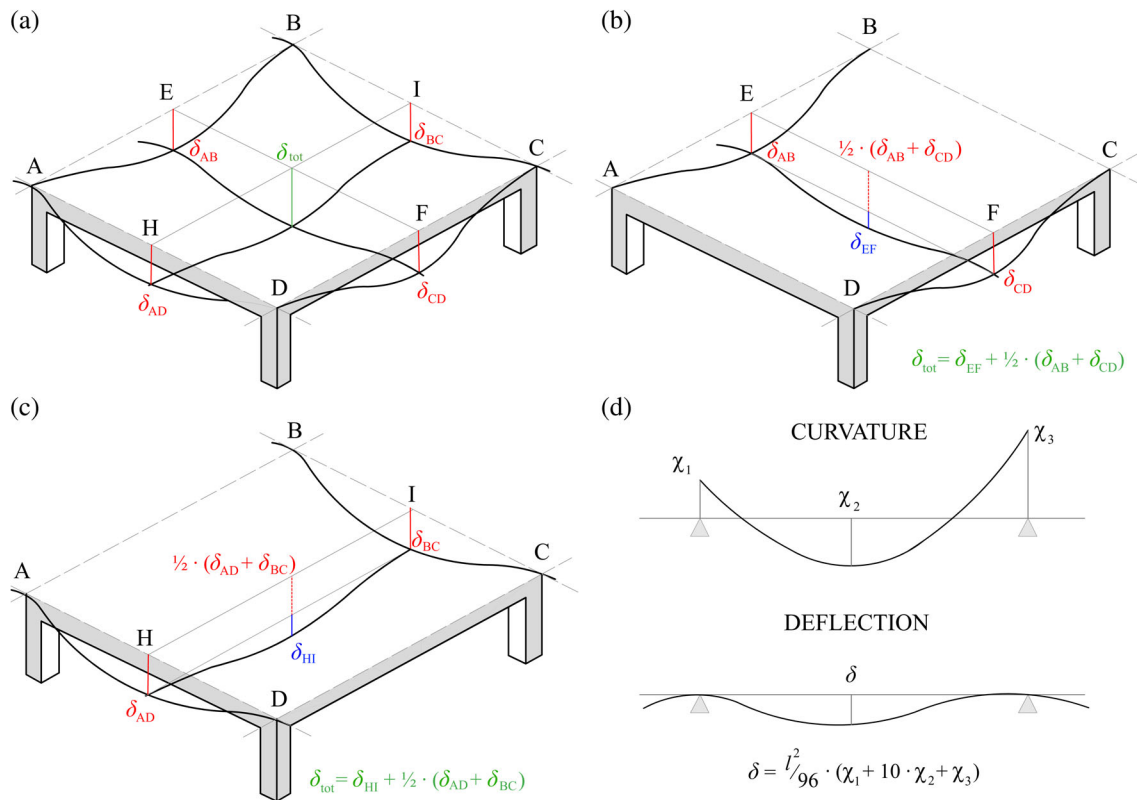
FIGURE 8 (a) Deflected shape of column-supported flat slab; (b,c) deflection at the centre of a rectangular panel; and (d) deflection-curvature relationship for column and middle strips (adapted from Reference 72)

Having calculated a distribution of moments (Figure 5c), the total instantaneous deflection at the center of certain panel (δ_{tot}) can be computed as the sum of the average deflection of two parallel column strips and the deflection of the middle strip spanning at right angle to the column strips (Figure 8b or Figure 8c). Among the possible approaches to assess the deflections of these strips, the procedure proposed by Ghali et al.[72,79] was found to be convenient for HRC solutions owing to the assumption that the variation of curvature follows a second degree parabola for the continuous straight members and, therefore, can be easily defined as per Figure 8d. As a result, this method is based on defining between six and nine curvatures depending on the symmetry of the bay considered.

Moreover, the mid-span sections can be referred to as the "determinant" sections (representing the stiffness of the zone exposed to positive bending moments and having the largest overall effect on deflections), and thus, the simplified approach permits[72,79] to evaluate the influence of cracking on the produced curvatures only in these sections, i.e., curvatures at the end sections can be studied as per homogenous material with established properties (moment of inertia and modulus of elasticity). In case of

RC solutions, the curvatures of "determinant" sections can be computed considering two extreme states: the uncracked condition in which concrete and steel are assumed to behave elastically and exhibit compatible deformations, and the fully cracked condition with the concrete in tension ignored.[79] Thereafter, the mean value of curvatures is to be obtained by means of interpolation. Adapting this approach to HRC solution, the section model described previously (Figure 6) along with the multi-layer sectional approach (inverse analysis)[80] may be applied to estimate the curvatures at the governing sections subjected to the given bending moments with further evaluation of the produced deflections in accordance with Figure 8d.

3 | DETAILS OF CASE STUDY

3.1 | Geometry and reinforcement layout

The selection of the geometry for the case study was oriented to reproduce common dimensions of slab panels that could be representative for office and residential buildings. Additionally, the number of three successive panels in each direction was chosen in order to involve
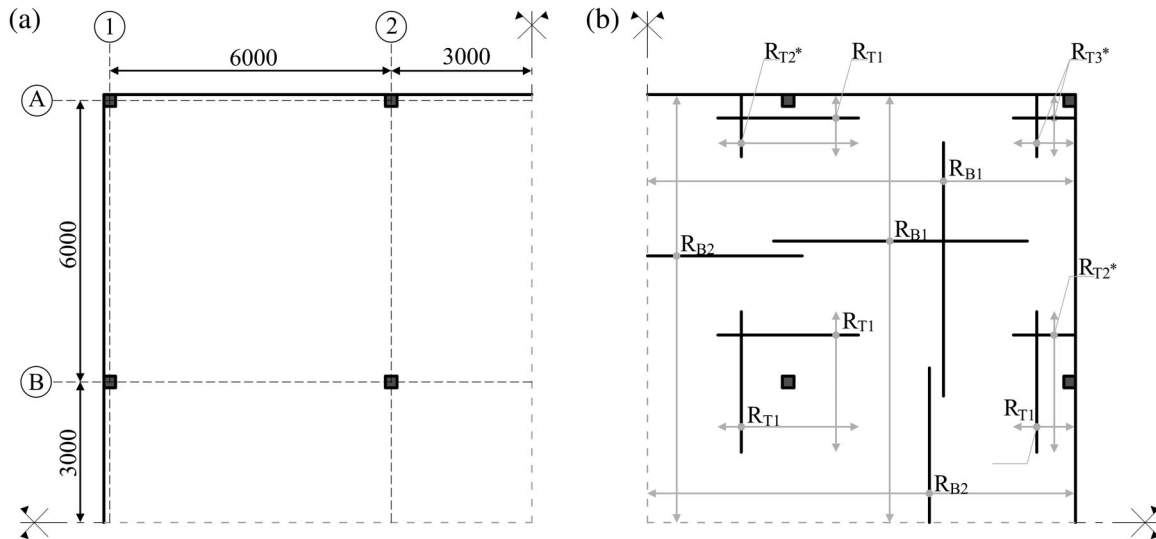
FIGURE 9   Analyzed HRC flat slab: (a) geometry and (b) reinforcement layout

into the analysis both corner and internal panels. Moreover, the FRC slabs of nine panels had been previously tested, which permitted carrying out a numerical validation of the model for the structure of the same geometry (Section 5.1). As a result, an $18.3 \times 18.3 \times 0.2$ m^3 slab supported by 16 columns with square cross sections of 0.3 m was analyzed. The uniform column grid (Figure 9a) formed nine panels of 6.0 x 6.0 m^2 each.

The reinforcement layout (Figure 9b) was adopted taking into consideration the advantages of using YLM for flat slabs: the bottom reinforcement (R_{B1}, R_{B2}) may be placed across whole bays, generally without curtailment. The top reinforcement (R_{T1}, R_{T2*}, and R_{T3*}, Figure 9b) was concentrated in the vicinity of columns in order to enhance the structural response at service loads in accordance with following ratios: the areas of $0.5 \cdot L_x \times 0.5 \cdot L_y$, $0.5 \cdot L_{x/y} \times (0.2 \cdot L_{y/x} + \text{E.D.})$, and $(0.2 \cdot L_x + \text{E.D.}) \times (0.2 \cdot L_x + \text{E.D.})$ were, respectively, placed over the internal, edge, and corner columns—E.D. in the presented expressions was equal to the distance between the centreline of column to edge of the slab, i.e., edge distance. Additionally, the selected types of reinforcement R_{T2*} and R_{T3*} should be explained: YLM suggests to provide similar positive and negative bending capacities to sections at the vicinity of columns once the possible local failures are to be analyzed; therefore, the "U" bars were provided in these zones.

The top reinforcement between concentrations over column heads is omitted—this approach can be applied even for RC solution,[47] even though cracking can develop in these areas (with minor effect on the structural performance). In case of HRC solutions, the possibility of cracking is significantly reduced due to presence of fibers. However, when necessary, the need of cracking-control

mesh in the above discussed zones can be assessed: the minimum reinforcement for the crack control may be estimated in accordance with the Clause 7.7.4.3 of the *fib* MC 2010.[19]

3.2 | Design actions

The loads specified in the Spanish Building Code for residential buildings[81] were considered as a reference to compute load combinations for both ULS and SLS. Apart from the self-weight (q_{SW}) of 4.8 kN/m^2, a dead load (q_G) and variable load (q_Q) of 2.0 and 3.0 kN/m^2, respectively, were assumed. Load partial safety factors $\gamma_G = 1.35$ and $\gamma_Q = 1.50$ were assumed to evaluate the design load at ULS: $q_{Sd} = \gamma_G \cdot (q_{SW} + q_G) + \gamma_Q \cdot q_Q = 13.7$ kN/m^2. The quasi-permanent load combination ($q_{k,\psi 2} = q_{SW} + q_G + \psi_2 \cdot q_Q$; $\psi_2 = 0.3$) for residential and office buildings was adopted for deflection and crack control checks. In the present study, this load combination resulted in a UDL of 7.7 kN/m^2.

3.3 | Material properties

Two different types of FRC were analyzed in the presented study for a more comprehensive analysis. FRC of 3c and 4d strength classes were selected—both types of concrete fulfilled the established requirements to be capable of substituting conventional reinforcement at ULS in accordance with the *fib* MC 2010: $f_{R1k}/f_{Lk} > 0.4$ and $f_{R3k}/f_{R1k} > 0.5$.[19] Table 2 gathers all mechanical properties of the selected materials which were considered in both analytical and numerical design procedures.

TABLE 2 Mechanical properties of FRC used in the design procedure

	E_c (MPa)	f_{ck} (MPa)	f_{cm} (MPa)	f_{ct} (MPa)	f_{R1k} (MPa)	f_{R3k} (MPa)	f_{R1m} (MPa)	f_{R3m} (MPa)
FRC3c	32,700	50.0	58.0	4.1	3.0	3.0	5.1	5.1
FRC4d	32,700	50.0	58.0	4.1	4.0	4.7	6.0	7.0

TABLE 3 Mechanical properties of reinforcing steel used in the design procedure

	E_s (GPa)	f_{yk} (MPa)	f_{tk} (MPa)	f_{ym} (MPa)	f_{tm} (MPa)	ε_{yk} (‰)	ε_{ym} (‰)	$\varepsilon_{uk} = \varepsilon_{um}$ (%)
B500C	210	500	575	550	632	2.4	2.6	10

The magnitudes of the compressive strength and modulus of elasticity were adopted based on the experimental campaign which involved the analysis of 15 self-compacting FRC mixes with fiber content up to 120 kg/m³ in order to establish suitable material for the construction of full-scale SFRC flat slab.[82] The mean values of the residual tensile strengths (f_{R1m}, f_{R3m}) were established by (1) assuming the normal distribution of f_R and (2) imposing values of the coefficient of variation (CV_{fR}) for the latter. In this regard, taking into consideration the extensive experimental programme[83] and values of CV_{fR} derived from a numerical study on the intrinsic scatter of FRC,[84] CV_{fR} of 25.0% and 20.0% were assumed for FRC3c and FRC4d, respectively.

The presented residual tensile strengths were not sufficient to provide the required bearing capacity of the structure in question. Therefore, the reinforcing steel B500C (classification was taken from the *fib* MC 2010,[19] Clause 5.2) was assumed for the reinforcing bars (Table 3). The numerical analysis also demands the mean yield/tensile strengths of steel to compute the global safety factor (Section 6.1); for this purpose, the established characteristic values were increased by 10% in conformity with the *fib* MC 2010 and EC2.[19,85]

4 | IMPLEMENTATION OF THE PROPOSED METHOD

4.1 | Required flexural capacity

Based on YLM along with the established design UDL at ULS and selected geometry, the maximum design bending moments can be computed for both corner and internal panels by means of Equations 1 and 2. For this purpose, the ratio of negative to positive flexural capacities ($\oslash_h$) was considered as 1.0. Additionally, the distance between the negative yield line and the centreline of external columns was adopted as 5.85 m for the corner panels and spacing between two negative yield

TABLE 4 Loads transferred to columns

Columns	A1	B1, A2	B2
Load (kN)	95	221	573

TABLE 5 Required amount of reinforcement

	$A_{s,req}$ (mm²/m)	
Reinforcement type	FRC 3c	FRC 4d
R_{B1}	382	283
R_{B2}	206	106
R_{T1}	804	592
R_{T2*}	331	233
R_{T3*}	328	230

lines for the internal panels (Figure 1) was assumed to be 5.70 m.

As a result, $m_{Ed,YL}^+ = m_{Ed,YL}^- = 40.2$ and 27.8 kNm/m for corner and internal panels, respectively (the detailed calculations can be found in the Supporting Information available with the online version of the article, Appendix S1). Thereafter, the flexural strengths of FRC 3c and FRC 4d were calculated by using the sectional model presented in Figure 3 followed by (1) distribution of the negative moments (Equation 7) and (2) assessment of the required amount of reinforcement in order to provide the sufficient bearing capacity demanded by the global failure mode. Finally, the local failure mode was analyzed; for this purpose, the loads transferred to each column from the slab tributary areas (under UDL of 13.7 kN/m²) were calculated (Table 4), this permitting to check the already computed reinforcement and to estimate the reinforcement for the edge and corner columns by Equation 3.

Table 5 presents the required amount of reinforcing steel bars for both FRC 3c and FRC 4d in accordance with the reinforcement layout depicted in Figure 9b; the

rebar detailing was not provided and the same amount of reinforcement per meter was used in the nonlinear analysis (Section 5.2) in order to carry out a more accurate comparison.

4.2 | Crack control at SLS

Firstly, the simplified elastic distribution of moments at ULS was evaluated by means of DDT (Figure 10). Table 6 reports the coefficients assumed to distribute the total static moment ($M_0 = q_u \cdot L_y \cdot L_n^2/8$) to supports and mid-span for negative moments and positive moments, respectively. Table 7 gathers the information regarding the distribution of the negative and positive moments transversely to the column and middle strips.
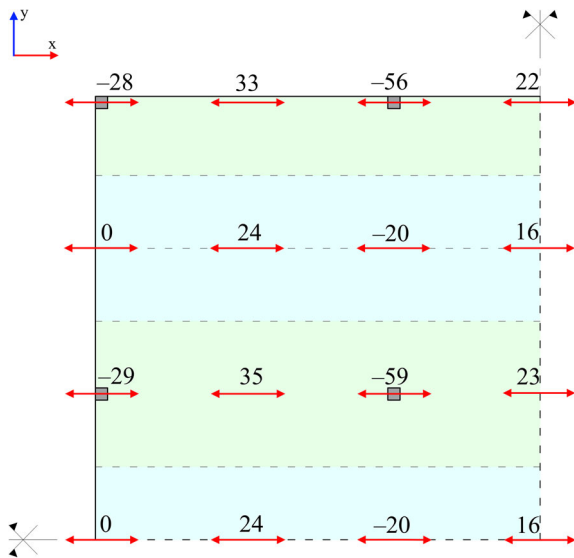

FIGURE 10 Bending moments (Mx) in design sections at ULS; values are presented in kNm/m

Additionally, the obtained values should be modified in accordance with EC2[42] to indirectly guarantee the cracking control (Figure 5d, Section 2.2.1)—the internal column B2 is taken as reference: 50% of the full negative moment from the sum of the two half panels (118.5 kNm) should be established in a width equal to the sum of 0.125 times the panel width on either side of the column (1.5 m), resulting in the overall bending moment of 79 kNm/m. Considering the material properties reported in Tables 2 and 3, the RC section of 200 × 1000 mm requires 1117 mm^2 in order to provide the adequate flexural strength under the moment of this magnitude (taking into account the traditionally adopted partial factors at ULS; $\gamma_s = 1.15$, $\gamma_c = 1.5$).

Finally, the structural response of three section alternatives should be studied at SLS in terms of the stresses to which the most demanded steel rebars are subjected under the quasi-permanent load combination. These sections of 200 × 1000 mm differ only in the type of reinforcement: (1) RC section with 1117 mm^2 of steel reinforcing bars, (2) FRC 3c with 804 mm^2, and (3) FRC 4d with 592 mm^2 (Table 5).

The moment-steel stress relationship (Figure 11) was computed for the sections in question in order to provide better visualization of the structural response of the studied alternatives. The material properties gathered in Tables 2 and 3 (represented by mean values) along with the constitutive model depicted in Figure 6 were taken into consideration for the sectional analysis. As a result, the influence of the bending moment on the steel stresses was estimated by varying the magnitude of the bending moment from 30 to 90 kNm/m.

The structural response of the RC section can be a reference for the evaluation of HRC solutions as it should ensure the sufficient cracking control of the studied two-way slab subjected to the previously described loads according to EC2.[42] The better performance of FRC 3c

TABLE 6 Distribution of total static moment in design sections

	Negative moment		Positive moment
Flat slab	**External support (%)**	**Internal support (%)**	**Mid-span (%)**
Without edge beams	26	70	52
Exterior edge is restrained	65	65	35

TABLE 7 Distribution of design moments between strips

	Negative moment		Positive moment
Strips	**External support (%)**	**Internal support (%)**	**Mid-span (%)**
Column	100	75	60
Middle	0	25	40
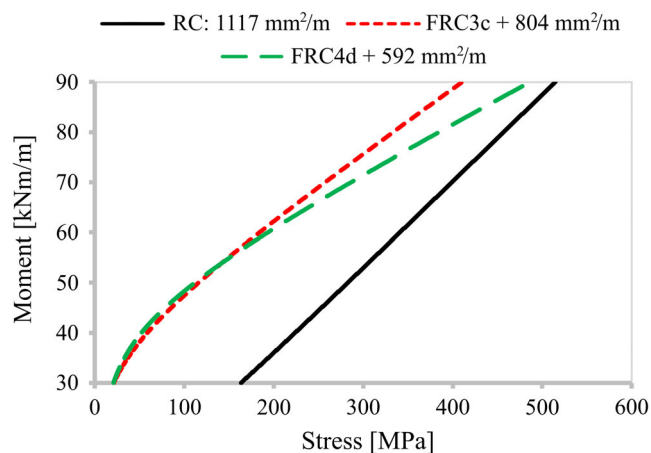
FIGURE 11 Moment–steel stress relationship of the studied sections

FIGURE 12 Bending moments (Mx, My) in design sections at (a) 7.7 kN/m^2 / (b) 17.0 kN/m^2; values are presented in kNm/m

+ 804 mm^2/m in comparison with the FRC 4d + 592 mm^2/m was expected because the relatively moderate postcracking residual flexural strength of FRC 3c permitted to concentrate negative moments in the vicinity of columns for the established top reinforcement layout, whereas FRC 4d tended to distribute the produced moments more evenly along the negative yield lines.

However, both solutions proved an enhanced behavior in terms of cracking control at SLS in comparison with the reference RC solution—the computed steel stresses (the factor of a significant effect on the crack width) were lower within the presented range of moments. Moreover, the steel stresses of FRC 3c + 804 mm^2/m and FRC 4d + 592 mm^2/m were lower to those of the RC solution (1117 mm^2/m) up to the yielding of the reinforcing steel bars. This fact guarantees the better performance of the HRC alternatives in terms of the required cracking control.

4.3 | Instantaneous deflections at SLS

The quasi-permanent load combination resulted in a UDL of 7.7 kN/m^2. The flexural moments in column and middle strip under this magnitude of UDL can be estimated by reducing (proportionally) those computed for ULS (Figure 10). Figure 12 presents the magnitudes of the bending moments to evaluate the instantaneous deformation in the centre of the corner panel. For this purpose, the deflections of two column strips in X direction (AB, CD) and the deflection of the middle strip at right angle to the column strips (EF) are to be calculated.

It is important to remark that only two of the bending moments presented in Figure 12 exceeded the cracking moment ($m_{cr} = f_{ct} \cdot b \cdot h^2 / 6 = 27.1$ kNm/m)—this is owed to the selected concrete mix, i.e., the required self-
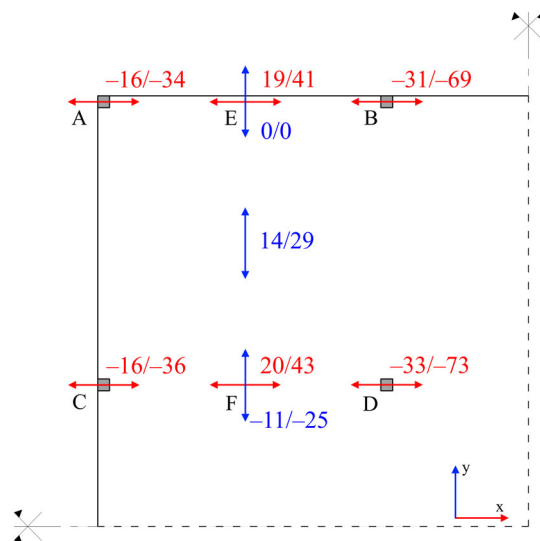
compacting behavior of FRC demands the increased content of cement and fine aggregates along with the additives (to reduce the water–cement ratio) as it was evidenced in.[8,82] These modifications lead to the increment of the material tensile strength which, in turn, can be beneficial in terms of serviceability performance; especially, considering that RC solutions for the flat slabs are usually designed/constructed with concrete classes C25–C30 (classification was taken from the fib MC 2010,[19] Clause 5.1.2).

From a design perspective, the increased concrete tensile strength favors the use of a simplified approach to calculate the produced deformations—less cracking tends to keep at a certain degree the elastic distribution of moments, i.e., cracking of the slab would lead to moment redistribution and, thereby, it would have an effect on deflections. Therefore, a traditional linear elastic analysis will produce a minor error.

Taking this into account, the elastic analysis was also carried out and compared with the results obtained by means of the adopted simplified method and NLFEA (Section 5.2). Realizing that the produced deformations should not differ significantly for a UDL of 7.7 kN/m^2, it was decided to extend the study and estimate the instantaneous deformations up to a UDL of 17 kN/m^2 (Figure 12) by means of the elastic analysis and the proposed method in order to: (1) compare in more detail the computed output with the NLFEA and (2) to prove the possibility of evaluating the required ductility in bending of FRC / HRC column-supported flat slabs by the proposed method.

The abovementioned requirement, in accordance with the fib MC 2010,[19] must satisfy at least one of the following conditions: (1) $\delta_u \geq 20 \cdot \delta_{SLS}$ and (2) $\delta_{peak} \geq 5 \cdot \delta_{SLS}$, where δ_u is the displacement corresponding to the
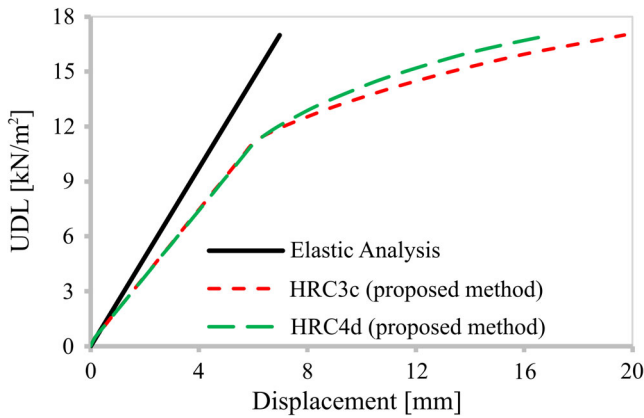
FIGURE 13 Structural response of studied HRC slab: UDL–displacement relationship

FIGURE 14 Considered finite element meshed model

ultimate capacity (P_u), δ_{peak} is the deflection at the maximum load (P_{max}), and δ_{SLS} is the displacement at SLS computed by performing a linear elastic analysis with the assumption of uncracked concrete. The assessment of δ_u by considering the elastic distribution of moments is excessively conservative due to the significant redistribution capacity of two-way HRC elements. However, it is possible to prove that the structure does not reach the maximum load at the displacement of $5 \cdot \delta_{SLS}$, augmenting the UDL and computing the produced deformations up to the required value ($5 \cdot \delta_{SLS}$) relying on the estimated curvatures.

As a result, the UDL-displacement relationship was estimated by means of elastic analysis (the software SAP2000[86] was used) and proposed method for both HRC solutions (Figure 13) varying the load from 0 to 17 kN/m². The produced displacement in the centre of the corner panel at SLS (UDL of 7.7 kN/m²) is 3.2 and 4.2 mm according to the elastic analysis and proposed method, respectively—these values are to be compared with the NLFEA output in the following sections. Additionally, it is important to remark that the proposed method evidenced sufficient ductility of the structural system: the displacement under the UDL of 17 kN/m² (with the capability of further load increment) was found to, respectively, be 19.7 and 17.0 mm for HRC 3c (FRC 3c + reinforcing bars) and HRC 4d (FRC 4d + reinforcing bars), whereas $5 \cdot \delta_{SLS} = 16$ mm.

5 | NUMERICAL MODELING

5.1 | Model validation

The finite element software ATENA 5.7.0[87] was used to model the structure under study, considering both hybrid alternatives. The structural response of FRC in tension
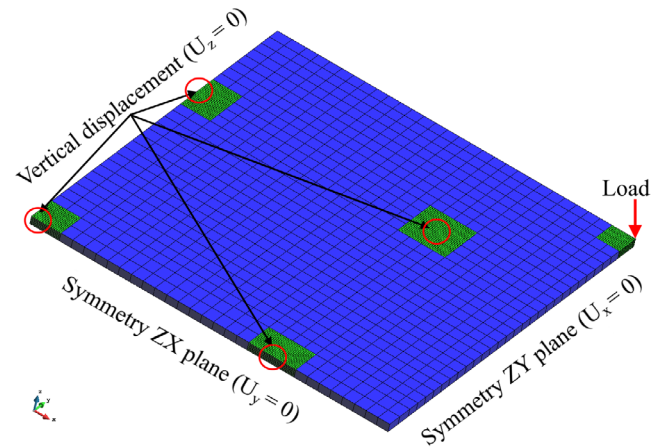
was reproduced by means of the multi-linear constitutive diagram depicted in Figure 6 which was based on the mechanical properties of the selected materials (Table 2). The compressive behavior of concrete was modeled using the stress–strain relationship for short-term loading in accordance with the Clause 5.1.8.1 of the *fib* MC 2010.[19] The behavior of steel was represented by the bilinear constitutive diagram following the Clause 3.2.7 of EC2[42] and taking into account the mechanical properties of reinforcing steel (Table 3).

The geometry of the HRC column-supported flat slab was modeled by means of 3D shell and solid elements—almost the entire structure was comprised of 3D shell elements considering that the analyzed element was mainly subjected to bending stresses; only the zones near the column-slab connections were modeled by solid 3D elements. Additionally, only a quarter of the studied element was modeled due to a double symmetry resulting in a total of 13,300 hexahedral elements (Figure 14). This approach required to impose the displacements in both symmetry planes. The column supports were reproduced by the rigid constraints in vertical direction—it is important to remark that the post-cracking tensile strength was increased in the regions above the columns (where vertical displacements were actually restricted) in order to properly reproduce the column-slab connection, avoiding the tensile local failures of these zones.

Before the verification of the proposed simplified method by means of NLFEA, the numerical model was validated by simulating two experimental tests[11,13] on full-scale column-supported flat slabs of the same geometry as that of the case study (Figure 9a). The first test was reported by Gossla,[11] which consisted in evaluating the structural response of the FRC slab (fiber content of 100 kg/m³) up to failure. The ultimate bearing capacity of the structure (named Bissen slab) was estimated by

means of the point load which was gradually applied in the centre of the element.

Prior to the full-scale test, the material characterization of the FRC considered was performed by means of four point bending test, square panel and round panel tests. The experimental outcome obtained by testing the round panels permitted to estimate the post-cracking behavior of FRC using the inverse analysis.[39] These properties ($f_{ct} = 2.5$ MPa, $f_1 = 1.75$ MPa, $f_2 = 1.06$ MPa, $f_3 = 0$ MPa and $w_{ct} = 0$ mm, $w_1 = 0.25$ mm, $w_2 = 1.25$ mm, $w_3 = 2$ mm), along with the information related to the measured compressive strength ($f_{cm} = 35$ MPa) and modulus of elasticity ($E_{cm} = 32,300$ MPa) were used in the simulation of the Bissen slab with minor modifications: ATENA permits to modify the pre- and post-cracking tensile models by means of stress–strain constitutive diagrams and, therefore, the presented crack widths were transformed to corresponding strains in

accordance with the crack band method and the smeared crack approach.[88]

The second FRC full-scale test (fiber content of 70 kg/m³, named Limelette slab) was tested under the same conditions up to failure—applying the point load at the centre of the slab. Therefore, only the material properties were reintroduced according to the information presented in the previous studies.[41,52] Post-cracking behavior was modeled considering the following tensile and residual tensile strengths at established crack widths: $f_{ct} = 2.2$ MPa, $f_1 = 1.2$ MPa, $f_2 = 1.2$ MPa, $f_3 = 0$ MPa and $w_{ct} = 0$ mm, $w_1 = 0.05$ mm, $w_2 = 1.5$ mm, $w_3 = 6$ mm, whereas the compressive strength and modulus of elasticity were adopted as 35 and 29,000 MPa, respectively. In both cases, the self-weight was imposed and then the point load was applied at a circular steel
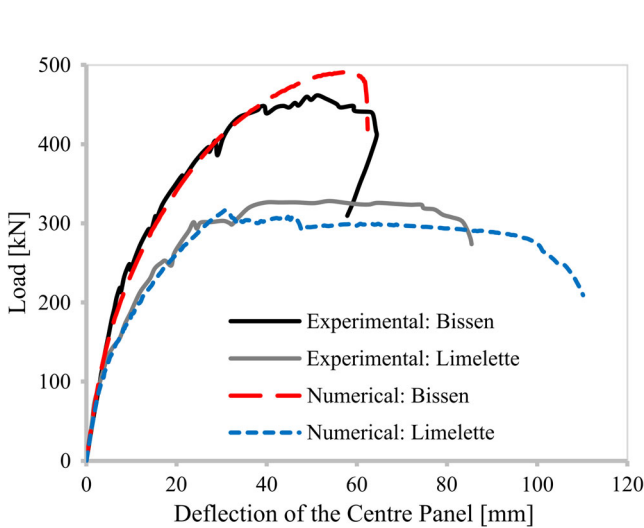

FIGURE 15 Experimental and numerical structural response of Bissen[11] and Limilette[13] full-scale tests
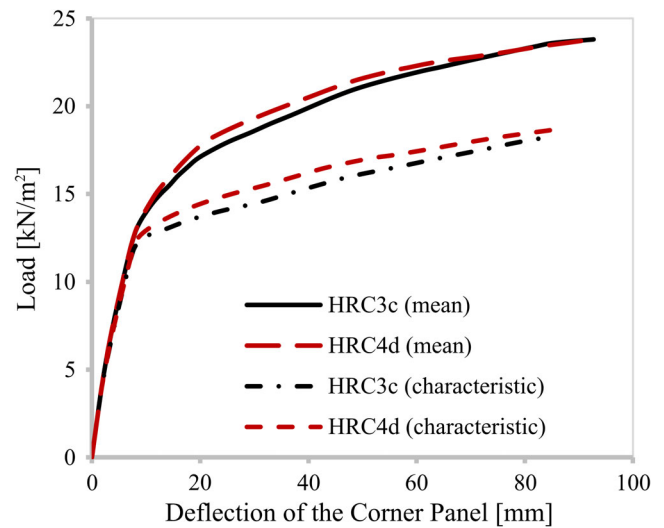

FIGURE 17 UDL (self-weight included)–deflection relationship for both HRC alternatives
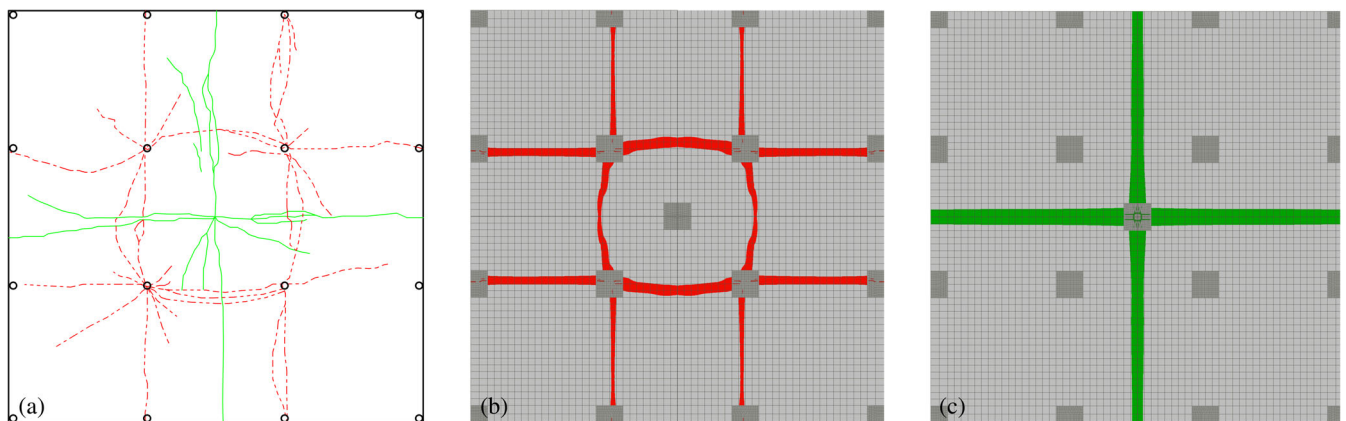

FIGURE 16 Produced crack patterns at ULS (red and green lines/areas indicate cracks at the top and bottom of the slab, respectively): (a) experimental test (adapted from Reference 52);(b,c) numerical prediction (the areas depict only the zones with $w_d > 1$ mm)

| Material | NLFEA | | | | | |
	R_m (kN/m^2)	R_k (kN/m^2)	γ_R	γ_{Rd}	R_d (kN/m^2)	E_d (kN/m^2)
FRC 3c	23.8	18.4	1.62	1.06	13.9	13.7
FRC 4d	23.8	18.7	1.56	1.06	14.4	13.7

TABLE 8 Global resistance of studied cases: mean, characteristic, and design values

plate of 20 mm of diameter by means of displacement control to guarantee the numerical convergence.

As a result, both simulations of the full-scale tests showed an accurate prediction of the structural behavior of FRC flat slabs tested experimentally (Figure 15). The computed maximum loads differed from those observed during the real testing by 6.3 and 3.6% in case of Bissen and Limelette slabs, respectively. Moreover, the simulations led to almost identical structural response up to deflections of 27 and 38 mm for the abovementioned FRC slabs—this aspect being of a paramount importance from the perspective of further analysis of the hybrid solutions at SLS. Additionally, the estimation of the developed cracks should be pointed out—considering that the crack patterns in both cases were similar, Figure 16 only presents the comparison of the produced cracks during the experimental test of the Limelette slab[13,52] with those predicted by the numerical simulation. Consequently, based on the obtained results, it can be stated that the numerical model was capable of predicting the structural response of the HRC solutions from low to high levels of applied loads.

5.2 | Modeling of HRC case studies

The geometry of Bissen and Limelette slabs was the same as that of the case study. Therefore, the previously described model (Figure 14) was used in order to analyze numerically the HRC alternatives with minor modifications—the one-dimensional reinforcing steel bars with a perfect bond were introduced to this model in accordance with (1) the established material properties (Table 3), (2) reinforcement layout (Figure 9), and analytical design output (Table 5). Additionally, the loading of the model was updated—the structure was subjected to the gradually increased UDL up to a failure. The failure criterion was related to the flexural response of the analyzed HRC column-supported flat slabs in terms of the produced deflections—further increment of UDL of 0.1 kN/m^2 should not have led to disproportionate deformations at the corner panel.

Figure 17 presents similar UDL-deflection relationship for studied HRC solutions using both mean and characteristic values of material properties, despite the differences of both residual tensile strengths and reinforcing steel bars amounts. Therefore, it can be concluded that, varying the residual tensile strength, the proposed simplified approach

based on the YLM permits to compute the required amount of the reinforcing steel bars, assuring almost identical structural response in flexure of HRC alternatives.

However, the next question that may arise is "Does this approach provide safe solutions in terms of design resistance?" To answer this question, the design global resistance of the structure was calculated in accordance with the *fib* MC 2010[19] (Clause 4.6.2.2) and compared with the initially established $q_{Sd} = 13.7$ kN/m^2.

6 | VALIDATION OF THE PROPOSED DESIGN METHOD

6.1 | Global resistance of the studied cases

The structural response of both HRC solutions was predicted (Figure 17) by nonlinear analysis using the mean values of selected material properties (Tables 2 and 3). Nonetheless, the global safety factor should be quantified by complying with the design condition (Equation 14). For this purpose, the method of estimation of a coefficient of variation of resistance (ECOV) was adopted.

$$E_d \le R_d = \frac{R_m}{\gamma_R \cdot \gamma_{Rd}} \tag{14}$$

$$V_R = \frac{1}{1.65} \ln \cdot \left(\frac{R_m}{R_k} \right) \tag{15}$$

$$\gamma_R = \exp(\alpha_R \cdot \beta \cdot V_R) \tag{16}$$

In this simplified probabilistic approach, the underlying assumption states that the coefficient of variation of resistance (V_R) can be assumed as lognormally distributed and can be expressed by means of Equation 15, i.e., may be estimated based on the mean (R_m) and characteristic (R_k) values of global resistance.[89] The computed coefficient of variation provides the possibility of evaluating the global safety factor (γ_R) using the Equation 16, which also takes into account the sensitivity factor (α_R) for the reliability of resistance and the reliability index (β). These two values (α_R, β) can be considered to be, respectively,
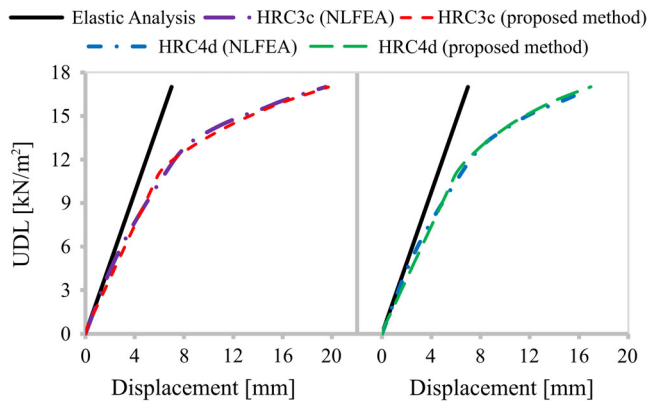
FIGURE 18 UDL–displacement relationship: NLFEA and proposed method

0.8 and 3.8 (for a service life of 50 years). Finally, the model uncertainty factor (γ_{Rd}) should be taken into account—the magnitude of the latter can be assumed to be 1.0, 1.06, and 1.1 for the models with no uncertainties, with low uncertainties and high uncertainties, respectively.[19] In the current study, the typically adopted value of 1.06 was assumed.

Applying the abovementioned approach, the global design resistance for the HRC alternatives was evaluated (Table 8). The design values of the global strength (R_d) are 1.4 and 4.8% higher than the required global resistance (E_d) for the alternatives FRC 3c and FRC 4d, respectively, i.e., the required flexural capacity was achieved by means of the proposed simplified method.

6.2 | Structural response of studied cases at SLS

The instantaneous deflections were computed by means of the developed approach (Figure 13). The numerical analysis, which was posteriorly conducted, permits to evaluate the accuracy of this approach. Figure 18 corroborates the precision of the proposed method—the estimated deflections at 7.7 kN/m^2 (quasi-permanent load combination) differ from those obtained numerically by 0.1 mm (2.4%). Moreover, the analytically assessed deflections were also in line with those calculated numerically up to the UDL which exceeded the established magnitude at ULS (13.7 kN/m^2).

Based on the abovementioned, the proposed method can be considered as suitable for verifying the ductility requirements in bending of the HRC alternatives. It must be highlighted that the numerical outcomes also allow confirming the viability of indirect method to guarantee the sufficient crack control since the maximum crack width at SLS is inferior to 0.3 mm, which is the

value generally established as a maximum crack width (w_{max}) for several exposure classes under quasi-permanent load combination of actions.[19,22,42]

7 | CONCLUSIONS

In this article, a design-oriented approach to evaluate the flexural capacity along with the estimation of instantaneous deflections and crack-width governing parameters is proposed for HRC column-supported flat slabs. Two HRC alternatives were studied by means of the proposed approach for a given geometry and boundary conditions. Additionally, a NLFE analysis was conducted in order to compare and validate the results obtained with the analytical approach. From this analysis, the following conclusions may be derived:

- The Yield Line Method permits to evaluate the overall flexural capacity of the HRC flat slabs with a possibility of distributing moments while accounting for the presence of FRC and HRC sections along the same yield line. Based on nonlinear analyses, the analytical approach provides a reliable results in terms of overall bearing capacity in flexure in case of the given structure subjected to UDL.
- The proposed approach, based on the crossing beam analogy along with indirect control of cracking for RC flat slabs, proved to be promising for dealing with the design at both SLS (crack width control and instantaneous deflection control).
- Additionally, the proposed method permits to check the ductility requirements for bending ($\delta_{peak} \geq 5 \cdot \delta_{SLS}$) by evaluating the expected deflections at ULS.

Even though the numerical analyses showed a considerable accuracy and precision of the proposed design-oriented approach, certain aspects are still to be studied for the consideration of this technological alternative (partial substitution of reinforcing steel bars by fibers in HRC flat slabs) by practitioners in the design phase. In this regard, the potential modification of the current FRC constitutive models for two-way elements, the estimation of the long-term behavior of FRC/HRC flat slabs, and the structural effect of induced holes into the slab are among the topics that should be further investigated. Furthermore, the parametric study which involves the variation of geometry, load type (UDL, point load) and magnitude of the latter can complement the presented investigation,

DATA AVAILABILITY STATEMENT

The datasets generated during and/or analysed during the current study are available from the corresponding author on reasonable request.

NOMENCLATURE

$A_{c,ef}$ — effective area of concrete in tension
A_s — area of reinforcement
b — section width
c — concrete cover
$CMOD$ — crack mouth opening displacement
d — section depth
E_c — modulus of elasticity of concrete
E — action–effect
E_s — modulus of elasticity of reinforcing steel
f_c — cylinder compressive strength of concrete
f_{ct} — axial tensile strength of concrete
f_{Fts} — serviceability residual strength for FRC
f_{Ftu} — ultimate residual strength for FRC
$f_{R,i}$ — residual flexural tensile strength of FRC corresponding to $CMOD_i$
f_y — yield strength of reinforcing steel in tension
f_t — tensile strength of reinforcing steel
h — overall depth of member
L — length
L_n — length of clear span
$L_{rx/y}$ — distance between two adjacent negative yield lines in a panel parallel to the x/y direction
$L_{x/y}$ — length of span in x/y direction
l_{cs} — characteristic length
$l_{s,max}$ — length over which the slip between steel and concrete occurs
m_E — value of applied moment
m_{cr} — cracking moment
m_R — value of resistant moment
q — uniformly distributed load
q_G — permanent load
q_Q — variable load
q_S — Combination of acting loads
q_{SW} — self–weight load
R — value of resistance
V_R — coefficient of variation of resistance
w — crack width
w_u — ultimate crack opening
x — depth of compression zone
α_e — modular ratio (E_s/E_c)

α_R — sensitivity factor
β — reliability index
γ_c — partial safety factor for concrete properties
γ_F — partial safety factor for FRC
γ_G — partial safety factor for permanent actions
γ_Q — partial safety factor for variable actions
γ_R — global resistance safety factor
γ_{Rd} — model uncertainty factor
γ_s — partial safety factor for reinforcing steel properties
δ — displacement
δ_{tot} — displacement at the centre of the panel
ε_{cm} — average concrete strain
ε_{cs} — shrinkage strain at concrete
ε_{sm} — mean steel strain
η_r — coefficient to consider the shrinkage contribution
ρ_s — ratio of tensile reinforcement
$\rho_{s,ef}$ — effective reinforcement ratio
σ_{sr} — steel stress in the crack under cracking load
τ_{bm} — mean bond strength between steel and concrete
χ — curvature
Ø_h — ratio of support to mid span moments
Ø_s — nominal diameter of bar
m — mean value of the variable
k — characteristic value of the variable
d — design value of the variable
FRC — fiber reinforced concrete
HRC — hybrid reinforced concrete
YL — yield line
σ_s — steel stress

ORCID

Stanislav Aidarov https://orcid.org/0000-0001-5576-7215
Nikola Tošić https://orcid.org/0000-0003-0242-8804
Albert de la Fuente https://orcid.org/0000-0002-8016-1677

REFERENCES

1. Blanco A, Pujadas P, de la Fuente A, Cavalaro SHP, Aguado A. Influence of the type of fiber on the structural response and design of FRC slabs. J Struct Eng. 2016;142(9):1–11. https://doi.org/10.1061/(ASCE)ST.1943-541X.0001515
2. di Prisco M, Colombo M, Pourzarabi A. Biaxial bending of SFRC slabs: is conventional reinforcement necessary? Mater Struct. 2019;52(1):1–15. https://doi.org/10.1617/s11527-018-1302-0
3. Facconi L, Minelli F, Plizzari G. Steel fiber reinforced self-compacting concrete thin slabs: experimental study and verification against model Code 2010 provisions. Eng Struct. 2016;122:226–37. https://doi.org/10.1016/j.engstruct.2016.04.030
4. Falkner, H. (2007). Steel fibre and polymere concrete basics, Model code 2007 and applications, pp. 381–400.
5. Fall D, Shu J, Rempling R, Lundgren K, Zandi K. Two-way slabs: experimental investigation of load redistributions in steel

fibre reinforced concrete. Engineering Structures. 2014;80:61–74. https://doi.org/10.1016/j.engstruct.2014.08.033

6. Michels J, Waldmann D, Maas S, Zürbes A. Steel fibers as only reinforcement for flat slab construction: experimental investigation and design. Construct Build Mater. 2012;26(1):145–55. https://doi.org/10.1016/j.conbuildmat.2011.06.004

7. Pujadas P, Blanco A, Cavalaro S, Aguado A. Plastic fibres as the only reinforcement for flat suspended slabs: experimental investigation and numerical simulation. Construct Build Mater. 2014;57:92–104. https://doi.org/10.1016/j.conbuildmat.2014.01.082

8. Aidarov S, Mena F, de la Fuente A. Structural response of a fibre reinforced concrete pile-supported flat slab: full-scale test. Engineering Structures. 2021;239:112292. https://doi.org/10.1016/J.ENGSTRUCT.2021.112292

9. Barros, J., Salehian, H., Pires, M. & Gonçalves, D. (2012). Design and testing elevated steel fibre reinforced self-compacting concrete slabs. Fibre Reinforced Concrete (BEFIB)

10. Destrée, X., & Mandl, J. (2008). Steel fibre only reinforced concrete in free suspended elevated slabs: case studies, design assisted by testing route, comparison to the latest SFRC standard documents. Tailor Made Concrete Structures, 437–443.

11. Gossla U. Development of SFRC free suspended elevated flat slabs. Aachen, Germany: Aachen University of Applied Sciences; 2005.

12. Hedebratt J, Silfwerbrand J. Full-scale test of a pile supported steel fibre concrete slab. Mater Struct. 2014;47(4):647–66. https://doi.org/10.1617/s11527-013-0086-5

13. Parmentier, B., Itterbeeck, P. van, & Skowron, A. (2014). The flexural behaviour of SFRC flat slabs: the Limelette full-scale experiments for supporting design model codes. In Proceedings of FRC.

14. Karv C. Shear and punching resistance of steel fibre reinforced concrete slabs. Espoo, Finland: Aalto University; 2017.

15. Mandl, J. (2008). Flat slabs made of steel fiber reinforced concrete (SFRC). In CPI worldwide.

16. Maturana Orellana, A. (2013). Estudio teórico-experimental de la aplicabilidad del hormigón reforzado con fibras de acero a losas de forjado multidireccionales. https://doi.org/10.1174/021435502753511268

17. Salehian H, Barros JAO. Prediction of the load carrying capacity of elevated steel fibre reinforced concrete slabs. Compos Struct. 2017;170:169–91. https://doi.org/10.1016/j.compstruct.2017.03.002

18. ACI Committee 544. (2004). Report on design and construction of steel fiber-reinforced concrete elevated slabs.

19. fib. (2010). fib Model Code for Concrete Structures 2010. www.fib-international.org

20. EV, DEUTSCHER BETON-UND BAUTECHNIK-VEREIN. DBV. Guide to Good Practice "Steel Fibre Concrete". Berlin: German Society for Concrete and Construction Technology; 2001.

21. Italian National Research Council CNR. CNR-DT 204/2006 Guide for the design and construction of fiber-reinforced concrete structures. Rome: Consiglio Nazionale Delle Ricerche; 2006.

22. Ministerio de Fomento. (2008). Instrucción de Hormigón Estructural (EHE-08). Boe N° 203. https://doi.org/10.1017/CBO9781107415324.004

23. RILEM TC 162-TDF. Recommendations of RILEM TC 162-TDF: test and design methods for steel fibre reinforced concrete—bending test. Mater Struct. 2002;35(253):579–82. https://doi.org/10.1617/14007

24. di Prisco M, Martinelli P, Dozio D. The structural redistribution coefficient KRd: a numerical approach to its evaluation. Struct Concr. 2016;17(3):390–407. https://doi.org/10.1002/suco.201500118

25. Maturana A, Canales J, Orbe A, Cuadrado J. Análisis plástico y Ensayos de Losas multidireccionales de HRFA. Inf Construc. 2014;66(535):e031. https://doi.org/10.3989/ic.13.021

26. Choi KK, Reda Taha MM, Park HG, Maji AK. Punching shear strength of interior concrete slab-column connections reinforced with steel fibers. Cem Concr Compos. 2007;29(5):409–20. https://doi.org/10.1016/j.cemconcomp.2006.12.003

27. Gouveia ND, Fernandes NAG, Faria DMV, Ramos AMP, Lúcio VJG. SFRC flat slabs punching behaviour: experimental research. Compos Part B Eng. 2014;63:161–71. https://doi.org/10.1016/j.compositesb.2014.04.005

28. Higashiyama H, Ota A, Mizukoshi M. Design equation for punching shear capacity of SFRC slabs. Int J Concr Struct Mater. 2011;5(1):35–42. https://doi.org/10.4334/ijcsm.2011.5.1.035

29. Ju H, Cheon NR, Lee DH, Oh JY, Hwang JH, Kim KS. Consideration on punching shear strength of steel-fiber-reinforced concrete slabs. Adv Mech Eng. 2015;7(5):1–12. https://doi.org/10.1177/1687814015584251

30. Kueres D, Polak MA, Hegger J. Two-parameter kinematic theory for punching shear in steel fiber reinforced concrete slabs. Eng Struct. 2020;205(2019):110086. https://doi.org/10.1016/j.engstruct.2019.110086

31. Maya LF, Fernández Ruiz M, Muttoni A, Foster SJ. Punching shear strength of steel fibre reinforced concrete slabs. Eng Struct. 2012;40:83–94. https://doi.org/10.1016/j.engstruct.2012.02.009

32. Nguyen-Minh L, Rovňák M, Tran-Quoc T, Nguyen-Kim K. Punching shear resistance of steel fiber reinforced concrete flat slabs. Proc Eng. 2011;14:1830–7. https://doi.org/10.1016/j.proeng.2011.07.230

33. Yang JM, Yoon YS, Cook WD, Mitchell D. Punching shear behavior of two-way slabs reinforced with high-strength steel. ACI Struct J. 2010;107(4):468–75. https://doi.org/10.14359/51663820

34. Barros JAO, Moraes Neto BN, Melo GSSA, Frazão CMV. Assessment of the effectiveness of steel fibre reinforcement for the punching resistance of flat slabs by experimental research and design approach. Compos Part B Eng. 2015;78:8–25. https://doi.org/10.1016/j.compositesb.2015.03.050

35. Tan KH, Venkateshwaran A. Punching shear in steel fiber-reinforced concrete slabs with or without traditional reinforcement. ACI Struct J. 2019;116(3):107–18. https://doi.org/10.14359/51713291

36. Gödde L, Mark P. Numerical simulation of the structural behaviour of SFRC slabs with or without rebar and pre-stressing. Mater Struct. 2015a;48(6):1689–701. https://doi.org/10.1617/s11527-014-0265-z

37. Nogales A, de la Fuente A. Numerical-aided flexural-based design of fibre reinforced concrete column-supported flat slabs. Eng Struct. 2021;232(2020):1–24. https://doi.org/10.1016/j.engstruct.2020.111745

38. Salehian H, Barros JAO. Assessment of the performance of steel fibre reinforced self-compacting concrete in elevated slabs. Cem Concr Compos. 2015;55:268–80. https://doi.org/10.1016/j.cemconcomp.2014.09.016

39. Soranakom, C., & Mobasher, B. (2007). Numerical simulation of FRC round panel tests and full-scale elevated slabs. ACI

Special Publication, 248(October 2014), 31–40. Retrieved from http://www.concrete.org/Publications/GetArticle.aspx?m=icap&pubID=19008

40. Teixeira MDE, Barros JAO, Cunha VMCF, Moraes-Neto BN, Ventura-Gouveia A. Numerical simulation of the punching shear behaviour of self-compacting fibre reinforced flat slabs. Construct Build Mater. 2015;74:25–36. https://doi.org/10.1016/j.conbuildmat.2014.10.003

41. Facconi L, Plizzari G, Minelli F. Elevated slabs made of hybrid reinforced concrete: proposal of a new design approach in flexure. Struct Concr. 2019;20(1):52–67. https://doi.org/10.1002/suco.201700278

42. EN 1992-1-1. (2004). Eurocode 2: Design of concrete structures: General rules and rules for buildings. Brussels: CEN. [Authority: The European Union Per Regulation 305/2011, Directive 98/34/EC, Directive 2004/18/EC]

43. Johansen KW. Brudlinieteorier. Denmark: København: Gjellerups; 1943.

44. Johansen KW. Yield-line theory. London: Cement and Concrete Association; 1962.

45. Johansen KW. Yield-line formulae for slabs. Boca Raton: CRC Press; 1972.

46. Gesund, H., & Dikshit, O. P. (1971). Yield line analysis of the punching problem at slab/column intersections. American Concrete Institute, ACI Special Publication, SP-030, 177–201.

47. Kennedy G, Goodchild CH. Practical yield line design. Surrey, UK: Concrete Centre; 2004.

48. Moss, R. M. (2001). Approaches to the design of reinforced concrete flat slabs. Construction Research Communications Limited by permission of Building Research Establishment.

49. CEN. (2007). EN 14651. Test method for metallic fibre concrete. Measuring the flexural tensile strength (limit of proportionality [LOP], residual).

50. ACI Committee 544. Guide for design with fiber-reinforced concrete. MI, USA: Farmington Hills; 2018.

51. Colombo M, Martinelli P, di Prisco M. On the evaluation of the structural redistribution factor in FRC design: a yield line approach. Mater Struct. 2017;50(1):1–18. https://doi.org/10.1617/s11527-016-0969-3

52. di Prisco M, Martinelli P, Parmentier B. On the reliability of the design approach for FRC structures according to fib Model Code 2010: the case of elevated slabs. Struct Concr. 2016;17(4):588–602. https://doi.org/10.1002/suco.201500151

53. Conforti A, Cuenca E, Zerbino R, Plizzari GA. Influence of fiber orientation on the behavior of fiber reinforced concrete slabs. Struct Concr. 2021;22(3):1831–44. https://doi.org/10.1002/suco.202000612

54. Leporace-Guimil B, Mudadu A, Conforti A, Plizzari GA. Influence of fiber orientation and structural-integrity reinforcement on the flexural behavior of elevated slabs. Eng Struct. 2022;252(2021):113583. https://doi.org/10.1016/j.engstruct.2021.113583

55. Blanco A, Pujadas P, Fuente A, Cavalaro SHP, Aguado A. Assessment of the fibre orientation factor in SFRC slabs. Composites B. 2015;68:343–54. https://doi.org/10.1016/j.compositesb.2014.09.001

56. Laranjeira F, Aguado A, Molins C, Grünewald S, Walraven J, Cavalaro S. Framework to predict the orientation of fibers in FRC: a novel philosophy. Cem Concr Res. 2012;42(6):752–68. https://doi.org/10.1016/j.cemconres.2012.02.013

57. Joint ACI-ASCE Committee 421. Guide to design of reinforced two-way slab systems. MI, USA: Farmington Hills; 2015.

58. Montoya, J., Meseguer, Á., Morán, F., & Arroyo, J. (2011). Hormigón Armado.

59. Jofriet JC. Flexural cracking of concrete flat plates. J Am Concr Inst. 1973;70(12):805–9. https://doi.org/10.14359/7139

60. Brotchie JF, Russel JJ. Flat Plate Structures I. Elastic-Plastic Analysis. Amer Concr Inst. 1964;61:959–96.

61. ACI. (2008). Control of cracking in concrete structures, ACI manual of concrete practice. ACI Committee 224, 224.2R-1-12.

62. ACI. ACI 318-14. Building code requirements for structural concrete. Farmington Hills: American Concrete Institute; 2014.

63. Nawy E. Crack control in reinforced concrete structures. ACI J Proc. 1968;65(10):825–36. https://doi.org/10.14359/7515

64. Orenstein G, Nawy E. Crack width control in reinforced concrete two-way slabs subjected to a uniformly distributed load. Am Concrete Inst J. 1970;67(1):57–61. https://doi.org/10.14359/7259

65. The Concrete Society. (2007). Technical report no. 64. Guide to the design and construction of reinforced concrete flat slabs. Camberley, UK.

66. Blanco A, Pujadas P, de la Fuente A, Cavalaro S, Aguado A. Application of constitutive models in European codes to RC-FRC. Construct Build Mater. 2013;40:246–59. https://doi.org/10.1016/j.conbuildmat.2012.09.096

67. Groli G, Caldentey AP. Improving cracking behaviour with recycled steel fibres targeting specific applications: analysis according to fib model Code 2010. Struct Concr. 2017;18(1):29–39. https://doi.org/10.1002/suco.201500170

68. Pujadas P, Blanco A, de la Fuente A, Aguado A. Cracking behavior of FRC slabs with traditional reinforcement. Mater Struct. 2012;45(5):707–25. https://doi.org/10.1617/s11527-011-9791-0

69. Tiberti G, Minelli F, Plizzari G. Cracking behavior in reinforced concrete members with steel fibers: a comprehensive experimental study. Cem Concr Res. 2015;68:24–34. https://doi.org/10.1016/j.cemconres.2014.10.011

70. Tošić N, Pecić N, Poliotti M, Marí A, Torres L, Dragaš J. Extension of the ζ-method for calculating deflections of two-way slabs based on linear elastic finite element analysis. Structural Concrete. 2021;22(3):1652–1670.

71. The Concrete Society. Technical report. Deflections in concrete slabs and beams. Volume No. 58. Camberley, UK: Concrete Society; 2005.

72. Ghali A. Prediction of deflections of two-way floor systems. ACI Struct J. 1989;86(5):551–62. https://doi.org/10.14359/3283

73. Beeby AW. A radical re-design of the in-situ concrete frame process, task 4: early striking of formwork and forces in backprops. London; CRC Limited; 2000.

74. Chang K-Y, Hwang S-J. Practical estimation of two-way slab deflections. J Struct Eng. 1996;122(2):150–9.

75. Kripanarayanan KM, Branson DE. Short-time deflections of flat plates, flat slabs, and two-way slabs. J Am Concr Inst. 1976;73(12):686–90. https://doi.org/10.14359/11107

76. Nilson AH, Walters DB. Deflection of two-way floor systems by the equivalent frame method. J Am Concr Inst. 1975;72(5):210–8. https://doi.org/10.14359/11132

77. Timoshenko S, Woinowsky-Krieger S. Theory of plates and shells. New York: McGraw-Hill; 1959.

78. Tošić N, Aidarov S, de la Fuente A. Systematic review on the creep of fiber-reinforced concrete. Materials. 2020;13(22):5098. https://doi.org/10.3390/ma13225098

79. Ghali A, Favre R, Elbadry M. Stresses and Deformations: Analysis and Design for Serviceability, 3rd ed. London: CRC Press; 1999.

80. Galeote E, Blanco A, de la Fuente A. Design-oriented approach to determine FRC constitutive law parameters considering the size effect. Compos Struct. 2020;239(2019):112036. https://doi.org/10.1016/j.compstruct.2020.112036

81. Gobierno de España. (2009). Código Técnico de la Edificación (CTE) Documento básico: Seguridad estructural. Apartado de "Acciones en la Edificación."

82. Mena, F., Aidarov, S., & de la Fuente, A. (2019). Hormigones auto-compactantes reforzados con fibras para aplicaciones con alta responsabilidad estructural. Campaña experimental en laboratorio. In III Congreso de Consultores de Estructuras (pp. 1–10).

83. Galeote E, Blanco A, Cavalaro SHP, de la Fuente A. Correlation between the Barcelona test and the bending test in fibre reinforced concrete. Construct Build Mater. 2017;152:529–38. https://doi.org/10.1016/j.conbuildmat.2017.07.028

84. Cavalaro SHP, Aguado A. Intrinsic scatter of FRC: an alternative philosophy to estimate characteristic values. Mater Struct. 2015;48(11):3537–55. https://doi.org/10.1617/s11527-014-0420-6

85. EN 1992–2. (2005). Eurocode 2: design of concrete structures: concrete bridges: design and detailing rules.

86. CSI. SAP2000 integrated software for structural analysis and design. Berkeley, CA: Computers and Structures Inc; 2021.

87. Cervenka V. Simulating a response. Concr Eng Int. 2000;4(4):45–9.

88. Červenka V, Jendele L, Červenka J. ATENA Program Documentation. Part 1: Theory. Prague: Cervenka Consulting sro; 2011.

89. Cervenka, V. (2013). Global safety formats in fib Model Code 2010 for design of concrete structures. In: 11th International Probabilistic Workshop, 31–40.

AUTHOR BIOGRAPHIES

Stanislav Aidarov; Smart Engineering Ltd. UPC Spin-Off, Jordi Girona 1-3, 08034 Barcelona, Spain. stanislav.aidarov@upc.edu

Nikola Tošić; Department of Civil and Environmental Engineering, Universitat Politècnica de Catalunya (UPC), Barcelona, Spain. Email: nikola.tosic@upc.edu

Albert de la Fuente, Civil and Environmental Engineering Department, Universitat Politècnica de Catalunya (UPC), Barcelona, Spain. Email: albert.de.la.fuente@upc.edu

SUPPORTING INFORMATION

Additional supporting information may be found in the online version of the article at the publisher's website.

How to cite this article: Aidarov S, Tošić N, de la Fuente A. A limit state design approach for hybrid reinforced concrete column-supported flat slabs. Structural Concrete. 2022. https://doi.org/10.1002/suco.202100785